A PETROLOGIC AND GEOCHEMICAL ANALYSIS OF THE MICA SCHISTS OF THE PTARMIGAN LAKE AREA, CENTRAL COLORADO

Matthew W. Owens
Department of Geology
The College of Wooster
Wooster, OH 44691

Outcrops around Ptarmigan Lake consist of Early Proterozoic (>1.6 b.y. old) interlayered mafic and felsic metavolcanics, pegmatites, migmatites, and mica schists. These are intruded by a poorly- to moderately well-foliated granodiorite pluton. Ptarmigan Lake is located in the Collegiate Peaks area of the southern Sawatch Range, 15 miles west of Buena Vista on the Cottonwood Pass Highway, Chaffee County Road 306, to County Road 346, and 3.3 miles up the Ptarmigan Lake trail; Mt Yale and Tincup 7.5 minute quadrangle.

The purpose of this study has been to sample the mica schists in the area, and to analyze them both petrographically and geochemically by X-ray fluorescence to determine their petrogenesis. Rock composition, grade of metamorphism, number of deformational events, possible source rock, and possible effects of the granodiorite intrusion are included in this analysis.

Twenty-nine samples of the mica schist were collected from roughly five outcrops around Ptarmigan Lake. Some of the samples were also taken from large blocks in the talus and glacial till to the north of the area along the Ptarmigan Lake trail. These samples still proved useful in the study as oriented samples were not being taken and metamorphic facies were not mapped. The author also aided in the compilation of a geologic map of the area.

Variations in composition and texture visible in hand sample were used as the basis for sample collection. Based on preliminary hand sample observation the schists consist of varying amounts of plagioclase, quartz, biotite, muscovite, sillimanite, and chlorite. Two populations of samples were identified based on the relative amounts of plagioclase, quartz, and micas. One population is more mica rich and is dark colored; referred to as the muscovite-sillimanite schists, while the other population is more plagioclase and quartz rich and is light colored; referred to as the quartzo-feldspathic schists.

Twenty-four chips for thin sections were cut while at Colorado College in Colorado Springs and were sent to Pioneer Thin Sections, Draper, Utah for manufacture. The chips were cut perpendicular to foliation; no lineation was seen in any samples in hand specimine. Point count analysis was performed on eight samples with an average of 320 grains counted per slide.

Samples were analyzed by X-ray fluorescence analysis at Franklin & Marshall College, Lancaster, PA with the help of Dr. Stanley Mertzman. Major and trace element analyses were done on eleven samples which were selected on the basis of sample location, amount of sample, and to which population the sample belonged. These analyses were plotted on various Harker diagrams and compared to plots of other lithologies (compositions found in literature) in order to determine a possible parent rock for the schists.

Petrographic analysis indicates that these schists are of the amphibolite grade of metamorphism and have undergone at least two periods of deformation. This is readily apparent by the presence of highly folded and sheared sillimanite, biotite, and muscovite grains producing a well aligned foliation, and large, undeformed muscovite grains growing at high angles to the foliation and across the deformed grains. The quartzo-feldspathic schists appear less sheared than the muscovite-sillimanite schists which may be due to the lesser amounts of platey and fiberous minerals, and the rock being more resistant to deformation. In thin section it is also noted that the schist contain not only plagioclase, quartz, biotite, muscovite, sillimanite, and chlorite, but also magnetite, hematite, sericite, and trace amounts of zircon, garnet, cordierite, and tourmaline. In some of the muscovite-sillimanite schists there are quartzo-feldspathic layers along some foliation planes. This may support the possibility of anatexis taking place prior to the second deformational event as large undeformed muscovites are also seen growing across these features.

The identification of muscovite-sillimanite and quartzo-feldspathic populations is in agreement with the findings in thin section. Seventeen of the twenty-four thin section samples are of the muscovite-sillimanite schist type while seven were of the quartzo-feldspathic schist type. This observation was made independent of the chemical analyses but again the two distinctions were found to be in full agreement. The results from point count analyses of eight samples also supports this distinction; four samples from both populations were counted. The quartzo-feldspathics contain 2 - 6% muscovite, 11 - 17% biotite, 24 - 37% plagioclase, 35 - 39% quartz, and an average of 3% sillimanite. The muscovite-sillimanite schists contain 25 - 54% muscovite, 12 - 20% biotite, 10 - 15% plagioclase, 9 - 20% quartz, and an average of 5% sillimanite.

Some interesting points about the chemical analyses are the high Al_2O_3 and K_2O values, and the inverse relationship of SiO_2 and Al_2O_3 (fig. 1). Plots of such rocks as shales, slates, graywackes, lutites, other mica schists, and weathered gneiss and diabase (compositions found in literature) were compared to those of these schists to try and explain these values and to determine a source rock (fig. 2). It was found that shales, slates, and weathered gneisses roughly match the area of the plotted quartzo-feldspathic schists but do not exhibit the inverse relationship between SiO_2 and Al_2O_3 or the high values of Al_2O_3 of the muscovite-sillimanite schists (Clarke, 1924; Goldich, 1938; Nanz, 1953; Pettijohn, 1975). The lithologies that comes closest in the plots of Al_2O_3 vs. SiO_2 are the weathered gneiss samples (Goldich, 1938), shales (Clarke, 1942; Pettijohn, 1975), and the lutites (Nanz, 1953).

There are a few possible answers to the anomalous compositions found in these schists. One is that the source was a weathered sediment or aluminum rich clay, shale, or soil. Another possibility is the occurrence of some form of metasomatism or anatexis, the exact nature of which is difficult to determine. The quartzo-feldspathics could be the results of the granodiorite intrusion and a more quartz-rich fluid moving from the pluton into the schists. This could explain the large muscovites growing across the foliation which would require larger amounts of water than are expected to have remained in the rock after this grade of metamorphism. Or the aluminum rich schists may be the residuum of anatexis removing quartz and plagioclase, which could represent the quartzo-feldspathic schists and the pegmatites and migmatites in the area, and leaving the micas and sillimanite behind.

References

Clarke, F.W., 1924, The data of geochemistry, 5th ed.: U.S. Geol. Surv. Bull. 770, 841 p.

Goldich, S.S., 1938, A study in rock weathering: Jour. Geology, v. 46, no. 1, p. 17 - 58, 10 figs. incl. index map.

Nanz, R.H., 1953, Chemical composition of Precambrian slates with notes on the geochemical evolution of lutites: Jour. Geology, v. 61, p. 51 - 64.

Pettijohn, F.J., 1975, Sedimentary Rocks, 3rd ed., table 8.7, p. 274, Harper and Row, New York.

----------, 1967, Data of geochemistry, 6th ed.: Chapter S. Chemical composition of sandstones - excluding carbonate and volcanic sands: U.S. Geol. Surv. Prof. Paper 440-S, 21 p.

	A	B	C	D	E	F	G
1	Sample	PT-12-O	PT-15-O	PT-21-O	PT-22-O	PT-26-O	PT-33-O
2	SiO2 %	49.36	54.29	43.91	52.59	49.59	56.58
3	TiO2	1.04	0.99	1.04	0.94	1.22	0.86
4	Al2O3	23.08	21.07	28.48	21.73	22.2	20.76
5	Fe2O3T	12.35	11.08	13.15	11.17	12.99	10.24
6	MnO	0.15	0.07	0.15	0.13	0.09	0.11
7	MgO	2.81	2.7	2.63	2.71	2.91	2.58
8	CaO	0.43	0.84	1.97	0.77	0.29	0.69
9	Na2O	1.02	1.54	2.9	1.39	0.57	1.26
10	K2O	6.35	4.31	3.62	5.41	6.74	4.05
11	P2O5	0.06	0.06	0.07	0.05	0.05	0.12
12	LOI	2.64	2.98	2.21	2.62	2.98	3.1
13	Total	99.29	99.93	100.13	99.51	99.63	100.35
14							
15	Rb ppm	104.04	229.2	290.46	265.2	277.97	190.55
16	Sr	316.2	206.28	138.02	214.5	91.96	155.4
17	Ba	585	826	1618	1187	1488	956
18	Y	16.32	32.47	45.32	29.25	25.08	37
19	Zr	220.32	240.66	249.26	427.05	359.48	227.55
20	V	96	136	156	141	126	119
21	Ni	48.96	64.94	65.92	62.4	137.94	62.9
22	Cr	109	149	132	128	169	108

	H	I	J	K	L	M
1	Sample	PT-18-O	PT-30A-O	PT-30B-O	PT-32B-O	PT-34-O
2	SiO2 %	66.92	66.24	60.87	67.61	69.37
3	TiO2	0.68	0.79	0.82	0.76	0.84
4	Al2O3	14.98	16.04	16.68	16.02	12.89
5	Fe2O3T	7.2	6.81	7.94	6.46	7.99
6	MnO	0.09	0.11	0.13	0.08	0.12
7	MgO	1.77	1.81	3.08	1.53	2.09
8	CaO	1.63	2.53	4.12	0.75	0.99
9	Na2O	2.67	3.21	2.92	1.33	1.41
10	K2O	2.23	1.34	1.81	3.43	2.79
11	P2O5	0.1	0.03	0.13	0.08	0.1
12	LOI	1.78	0.92	1.08	2.71	1.29
13	Total	100.05	99.83	99.58	100.76	99.88
14						
15	Rb ppm	85.28	92.91	136.5	149.73	129.2
16	Sr	254.2	321.11	322	152.95	107.1
17	Ba	609	308	230	713	722
18	Y	13.12	27.71	22.75	16.1	22.1
19	Zr	180.4	221.68	159.25	236.67	243.1
20	V	94	66	80	83	93
21	Ni	42.64	44.01	71.75	35.42	52.7
22	Cr	108	103	115	105	152

Figure 1. Analyses of Ptarmigan Lake mica schists. Samples PT-12, 15, 21, 22, 26, and 33-O are muscovite-sillimanite schists. Samples PT-18, 30A, 30B, 32B, and 34-O are quartzo-feldspathic schists.

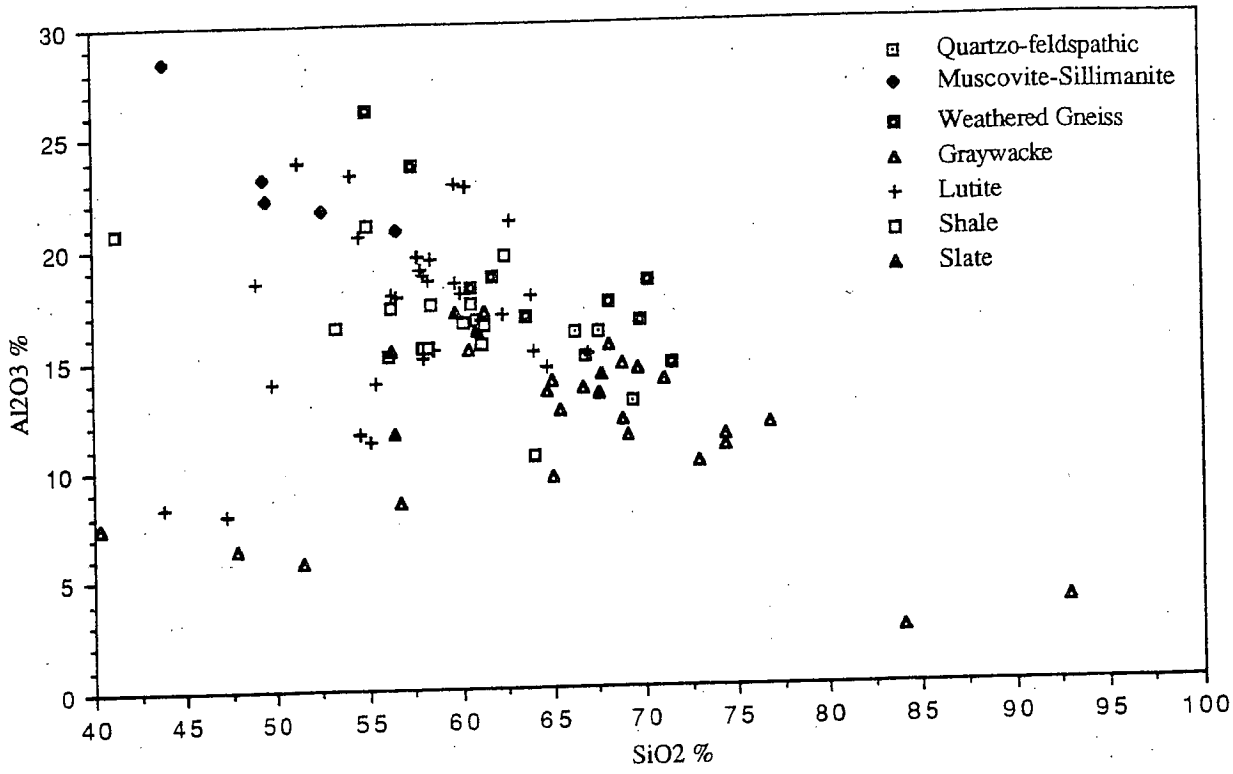

Figure 2. Comparative plot of Ptarmigan Lake mica schists and other lithologies: compositions from Clarke (1924), Goldich (1938), Nanz (1953), and Pettijohn (1967, 1975).

	A	B	C	D	E	F	G
1	Sample	PT-12-O	PT-15-O	PT-21-O	PT-22-O	PT-26-O	PT-33-O
2	SiO2 %	49.36	54.29	43.91	52.59	49.59	56.58
3	TiO2	1.04	0.99	1.04	0.94	1.22	0.86
4	Al2O3	23.08	21.07	28.48	21.73	22.2	20.76
5	Fe2O3T	12.35	11.08	13.15	11.17	12.99	10.24
6	MnO	0.15	0.07	0.15	0.13	0.09	0.11
7	MgO	2.81	2.7	2.63	2.71	2.91	2.58
8	CaO	0.43	0.84	1.97	0.77	0.29	0.69
9	Na2O	1.02	1.54	2.9	1.39	0.57	1.26
10	K2O	6.35	4.31	3.62	5.41	6.74	4.05
11	P2O5	0.06	0.06	0.07	0.05	0.05	0.12
12	LOI	2.64	2.98	2.21	2.62	2.98	3.1
13	Total	99.29	99.93	100.13	99.51	99.63	100.35
14							
15	Rb ppm	104.04	229.2	290.46	265.2	277.97	190.55
16	Sr	316.2	206.28	138.02	214.5	91.96	155.4
17	Ba	585	826	1618	1187	1488	956
18	Y	16.32	32.47	45.32	29.25	25.08	37
19	Zr	220.32	240.66	249.26	427.05	359.48	227.55
20	V	96	136	156	141	126	119
21	Ni	48.96	64.94	65.92	62.4	137.94	62.9
22	Cr	109	149	132	128	169	108

	H	I	J	K	L	M
1	Sample	PT-18-O	PT-30A-O	PT-30B-O	PT-32B-O	PT-34-O
2	SiO2 %	66.92	66.24	60.87	67.61	69.37
3	TiO2	0.68	0.79	0.82	0.76	0.84
4	Al2O3	14.98	16.04	16.68	16.02	12.89
5	Fe2O3T	7.2	6.81	7.94	6.46	7.99
6	MnO	0.09	0.11	0.13	0.08	0.12
7	MgO	1.77	1.81	3.08	1.53	2.09
8	CaO	1.63	2.53	4.12	0.75	0.99
9	Na2O	2.67	3.21	2.92	1.33	1.41
10	K2O	2.23	1.34	1.81	3.43	2.79
11	P2O5	0.1	0.03	0.13	0.08	0.1
12	LOI	1.78	0.92	1.08	2.71	1.29
13	Total	100.05	99.83	99.58	100.76	99.88
14						
15	Rb ppm	85.28	92.91	136.5	149.73	129.2
16	Sr	254.2	321.11	322	152.95	107.1
17	Ba	609	308	230	713	722
18	Y	13.12	27.71	22.75	16.1	22.1
19	Zr	180.4	221.68	159.25	236.67	243.1
20	V	94	66	80	83	93
21	Ni	42.64	44.01	71.75	35.42	52.7
22	Cr	108	103	115	105	152

Figure 1. Analyses of Ptarmigan Lake mica schists. Samples PT-12, 15, 21, 22, 26, and 33-O are muscovite-sillimanite schists. Samples PT-18, 30A, 30B, 32B, and 34-O are quartzo-feldspathic schists.

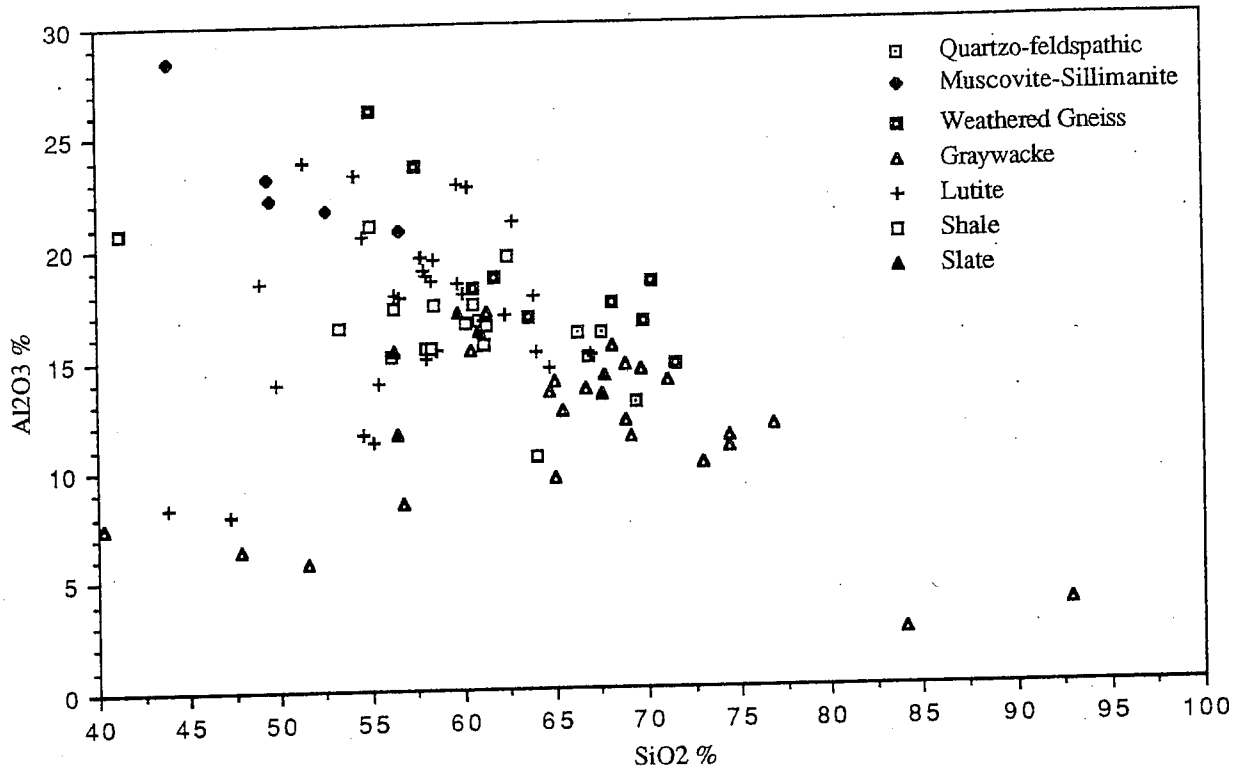

Figure 2. Comparative plot of Ptarmigan Lake mica schists and other lithologies: compositions from Clarke (1924), Goldich (1938), Nanz (1953), and Pettijohn (1967, 1975).